

# Photon mapping to accelerate daylight simulation with high-resolution, data-driven fenestration models

Lars O Grobe<sup>1,2</sup>

<sup>1</sup> Institute of Building Engineering, Lucerne University of Applied Sciences and Arts, Technikumstrasse 21, 6048 Horw, Switzerland

<sup>2</sup> Department of Architecture, Izmir Institute of Technology, Urla, 35430 Izmir, Turkey

E-mail: larsoliver.grobe@hslu.ch

**Abstract.** Data-driven modelling provides a general means to represent optically complex fenestration in daylight simulation by its Bidirectional Scattering Distribution Function (BSDF). RADIANCE employs the *tensor tree* as a compact data structure to store the BSDF at high directional resolution. The application of such models under sunny sky conditions is, however, computationally demanding, since the density of stochastic backward samples must match the BSDF resolution. The bidirectional PHOTON MAP is proposed to rapidly forward-sample the BSDF, starting from the known sun direction. Its exemplary application shows a potential speed-up of  $\geq 98\%$  when compared to backward ray-tracing.

## 1. Introduction

### 1.1. Data-driven modelling of complex fenestration

Optically complex, e.g. light redirecting, retro-reflecting, or directionally selective fenestration, is characterized by its irregular light scattering properties. Light transport between any pair of incident direction  $(\theta_i, \phi_i)$  and outgoing – scattered – direction  $(\theta_s, \phi_s)$  is described by the Bidirectional Scattering Distribution Function (BSDF). Data-driven fenestration models are discrete representations of the BSDF, such as dense matrices, comprising coefficients that evaluate to the radiative transfer through fenestration. Employed in building performance or daylight simulation, data-driven models encapsulate the fenestration's complexity. They can be generated either from measurements or by computational means [1, 2]. Models that combine 145 incident with 145 outgoing directions are successfully employed in the computation of integral quantities such as solar heat gain or illuminance. Since the corresponding angular resolution of  $\approx 10^\circ$  to  $15^\circ$  may be inadequate for luminance-based assessments of visual comfort, and glare in particular [3, 4], the *tensor tree* has been implemented in the light simulation suite RADIANCE as a memory-efficient data-structure of locally adaptive resolution [5]. On typical hardware, the tensor-tree supports resolutions of up to  $\approx 1.5^\circ$  for anisotropic, and  $\approx 0.4^\circ$  for isotropic scattering.

Given the high efficiency of the tensor-tree as a data-structure, sampling of the models becomes the limiting constraint in daylight simulation. Since the backward ray-tracing algorithm implemented in RADIANCE cannot predict which outgoing directions lead indirectly – via intervening scattering – to light sources, e.g. the sun, it relies on random sampling at a density that must match the resolution of the data-driven model. Such dense sampling drastically affects



performance. Two approaches have been developed to accurately replicate highly directional transmission even with data-driven models of moderate resolution. The *BSDF proxy* combines geometric with data-driven models [6]. It relies on the latter only in the stochastic calculation of diffuse inter-reflections. An accurate geometric description of the fenestration is required. *Peak extraction* analyses the BSDF to identify pairs of incident and outgoing directions, where direct transmission occurs [7]. For these pairs, a peak is synthesized independently from the BSDF's resolution. Peak shape and direction have to be known in advance. No method exists to avoid the impractically dense, stochastic sampling of the data-driven model, if neither system geometry nor peak shape and direction are known.

### 1.2. Photon mapping in daylight simulation

The problems of stochastic sampling of high-resolution BSDFs show similarity to the challenge of tracing rays toward the sun through geometric models of daylighting devices, that motivated the initial implementation of the bi-directional PHOTON MAP [8] in RADIANCE [9, 10]. It has been successfully integrated in the simulation and performance analysis software EVALDRC to assess daylight supply measured by the combined illuminance-based metrics spatial Daylight Autonomy (sDA) and Annual Sunlight Exposure (ASE) [11]. EVALDRC combines a coarse but efficient Daylight Coefficient (DC) calculation with a refined sun-model. The approach is similar to that of DAYSIM [12], but, other than the latter, supports data-driven BSDF models to describe irregular transmission. A recent modification of the PHOTON MAP implementation in RADIANCE extends the application of the software to image synthesis for visual comfort assessments, including Climate-Based Daylight Modelling (CBDM) techniques. The high number of light sources employed in refined sky models in CBDM must be matched by a sufficient number of photons attributed to each source. To accommodate the resulting growth of contribution photon maps, an Out-of-Core (OoC) data structure is employed that can be efficiently accessed through a spatially ordered *photon cache* [13].

### 1.3. Objectives

This research tests the efficiency of this modified PHOTON MAP module. For one time-step, generated imagery and simulation times are reported for

- backward ray-tracing, considered the reference algorithm,
- the PHOTON MAP with indirect visualization of global photons for improved image quality,
- with direct global photon visualization to accelerate image synthesis, and
- with direct photon visualization and precomputed global photons as the potentially faster rendering technique.

To demonstrate the applicability of the PHOTON MAP in CBDM, results of exemplary annual simulations for visual comfort assessment are presented.

## 2. Test case

A South-facing cellular office of dimensions width  $w = 2.75$  m, depth  $d = 5.95$  m, and height  $h = 3.20$  m features a fully glazed façade [1]. The inner surfaces of the room are ideally diffuse with direct-hemispherical reflectance of  $\rho_{d,h} = 0.20$  (floor),  $\rho_{d,h} = 0.50$  (walls), and  $\rho_{d,h} = 0.70$  (ceiling) respectively. The only permanently occupied work-desk is oriented toward the Eastern side-wall. The top surfaces of the light grey desk ( $\rho_{d,h} = 0.50$ ), and other furniture, are moderately glossy. Imagery is generated under sky conditions in Izmir, at the Aegean Sea in the West of Turkey.

Table 1: Symbols and distribution parameters for different photon types.

Description	Symbol	Target
Global	G	2M
Caustic	C	2M
Precomputed	P	2M
None (backward ray-tracing)	x	-

Table 2: Photon distribution (top row) and image generation (right column) times.

	G	C	P	$t(\text{rtpict})$
$t(\text{mkpmap})$	209.8 s	382.7 s	238.6 s	
xxx				103 116 s
GCx	+	+		1889 s
xCP		+	+	792 s
xxP			+	2320 s

### 3. Daylight simulation of one time-step employing the photon map

#### 3.1. Method

To test the efficiency of the PHOTON MAP with data-driven BSDF models, a model of the office is prepared with a Laser Cut Panel (LCP) installed in the upper window zones. The aim of this optically Complex Fenestration System (CFS) is to deflect incident light toward the ceiling, and to improve the uniformity of the illuminance distribution in the room especially under sunny sky conditions. The remaining fenestration area provides an unobstructed view to the outside.

The BSDF of a sample of the LCP was characterized on a scanning goniophotometer [14]. The measurement relies on an asymmetric directional resolution – the distribution of scattered light resulting from few incident directions is scanned at high directional resolution. For each incident direction, the measured outgoing distributions are approximated by sets of Radial Basis Functions (RBFs). A discrete, four-dimensional tensor representation of symmetric resolution is generated by interpolation between the RBFs corresponding to the three closest incident directions (assuming anisotropic scattering). Spatially adaptive data-reduction merges the elements of this tensor, resulting in a compact, hierarchical data-structure that accounts for distinct features of the BSDF. The generation of RBF interpolants, and subsequent discretization and data-reduction, is performed by the two programs `pabopto2bsdf` and `bsdf2ttree` as distributed with RADIANCE. The initial tensor of  $16\,384 \times 16\,384$  elements is reduced by 95%, and the BSDF model is applied to the glazing of the upper window zone.

Three photon maps with a target of 2 Mio photons each are generated (Table 1). *Global* photons (G) are stored whenever rays emanating from the light sources, here the sky and the sun, hit a diffuse surface. The *caustic* (C) photon map stores only those photons that collide with a diffuse surface immediately after a) mirror-like reflection, b) directional scattering (transmission or reflection), e.g. by the data-driven model, or c) regular (non-scattered) transmission if preceded by a) or b). Note that the caustic photon map is a sub-set of the global photon map. The density of global and caustic photons correlates with the illuminance on the surface they are deposited on. Finally, *pre-computed* global photons (P) are attributed an estimate of the local illuminance and accelerate the rendering process, since the local illuminance is accessible by the nearest pre-computed photon rather than the density of numerous global photons [15]. Photon distribution is performed by the program `mkpmap`. In typical applications, all photon maps would be generated in one pass and by parallel processes. In this research, to measure the individual time required for the tracing of different photon types, the photon maps are generated sequentially by one process under the assumption that the parallelized processes scale in relation.

Image synthesis is performed using `rtpict` by backward ray-tracing with up to four inter-reflections, and by replacing the diffuse inter-reflection calculation in parts or entirely by photon mapping. The combination of photon types is encoded in three-letter sequences as introduced in Table 2. All imagery is generated with at least one indirect-diffuse inter-reflection step to avoid the visual artefacts that occur when global photons are directly visualized.

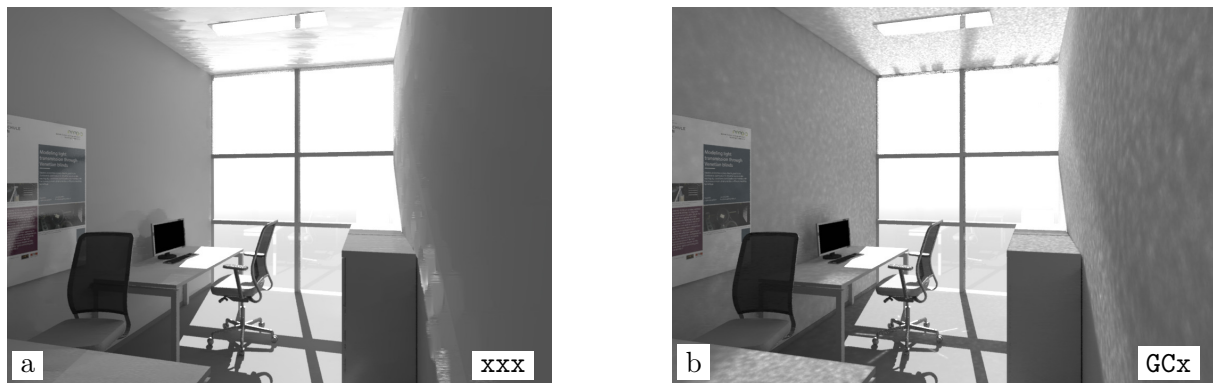


Figure 1: Result of backward ray-tracing (a) and the PHOTON MAP (b) for one time-step .

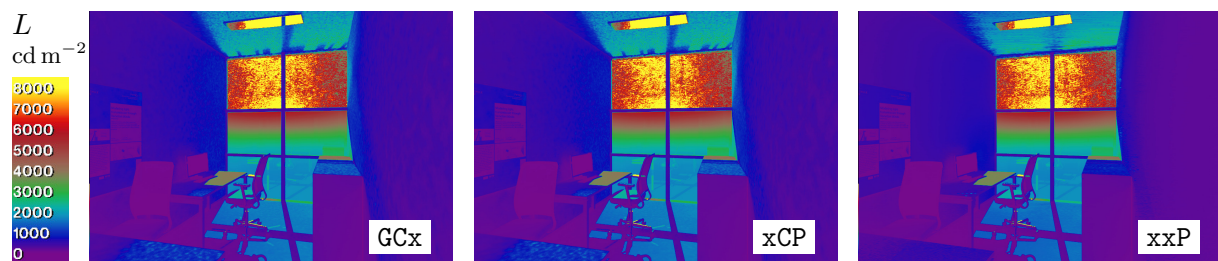


Figure 2: Falsecolor images generated by accelerated techniques employing precomputed photons.

### 3.2. Results and discussion

The processing times for each photon type are reported in Table 2. The top row shows the elapsed time during the generation of the three photon maps. The global photon map just records the given number of target photons, without discarding or further processing. The caustic photon aims to achieve the same target, but has to distribute more photons since only those meeting the criteria of caustics are recorded. Consequently, the processing time increases. The generation of the precomputed photon map is basically identical to that of the global photon map, with an additional photon gathering step accounting for a moderate increase of the processing time.

Figure 1 contrasts ray-tracing (a) with the parametrization of the PHOTON MAP optimized for highest image quality. The latter causes typical artefacts, such as *photon noise* of moderate frequency, and *bias* e.g. along the junction of walls and ceiling. Deflection of sun-light by the LCP is precisely replicated. Ray-tracing, on the other hand, shows the interpolation artefacts of the ambient cache, apparent e.g. as circular patterns on the right wall, and cannot replicate the sharp contours of upward deflected sun-light as accurately as the PHOTON MAP.

The right column of Table 2 lists the time required for image synthesis by ray-tracing, and by selective replacement of parts of the diffuse inter-reflection calculation by photon maps. All techniques employing the PHOTON MAP are faster than backward only ray-tracing. Compared to GCx, replacing the density estimate of nearest photons by precomputed photons xCP achieves a further acceleration by a factor of  $\approx 2.4$ . The exclusion of caustic photons in xxP leads to a performance decrease due to the added sampling of specular paths e.g. from the ceiling toward the sun, which the caustic photon map pre-computes in GCx and xCP. Figure 2 confirms that all techniques lead to comparable results other than a moderately underestimated brightness on the right wall and the desk in the foreground by xxP. Accounting for the glancing light received by the fenestration would require further refinement of the ambient sampling here by decreasing the ray weight parameter (which was set to  $1 \times 10^{-4}$ ) at the expense of increased simulation time.

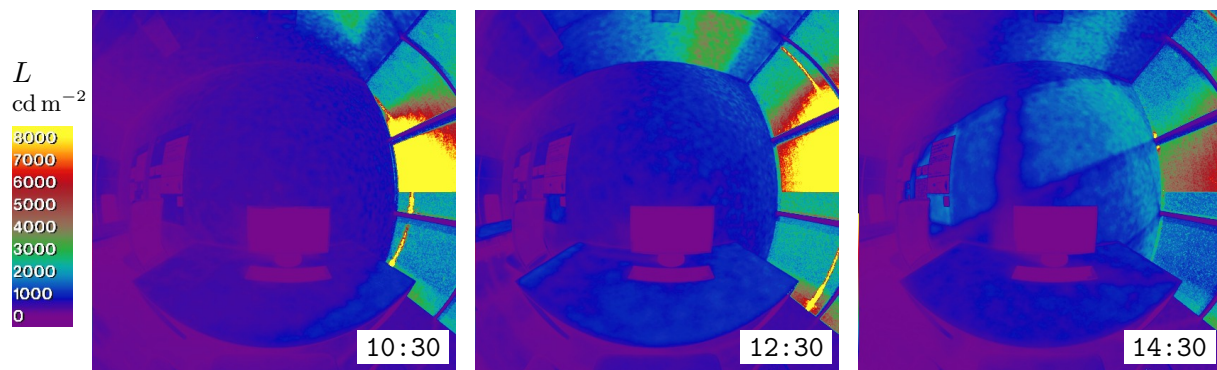


Figure 3: Image sequence by CBDM employing the PHOTON MAP, March 22. Note the vertical highlight in the fenestration at 10:30 and 12:30, and the upward deflection of sun-light.

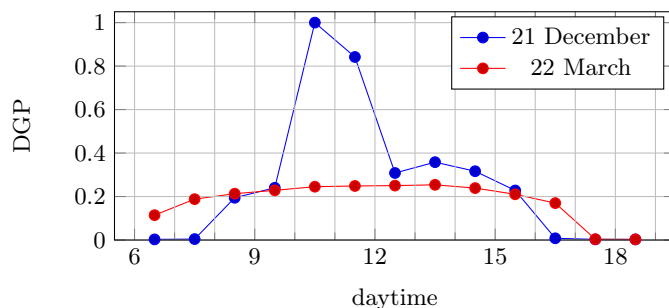


Figure 4: DGP computed from imagery generated by CBDM employing the PHOTON MAP, covering two exemplary days.

#### 4. Climate-Based Daylight Modelling (CBDM) employing the photon map

##### 4.1. Method

Due to its capability to efficiently generate imagery with data-driven BSDF models under sunny sky conditions, the complex calculation of the solar component in the Five Phase Method (FPM) is replaced by a DC calculation employing *contribution photons*. To account for each of the 5184 suns of a MF:6 *Reinhart discretization* by a sufficient number of photons, the OoC PHOTON MAP implementation is employed [13]. To leverage local proximity in subsequent photon look-ups for optimized use of the *photon cache*, photon are directly visualized, which increases photon noise. The diffuse sky, an extended source that is not efficiently accounted for by the PHOTON MAP, is modelled by a conventional Three Phase Method (TPM). Other than e.g. the FPM, the separate calculation of sky- and sun-light employing the PHOTON MAP does not depend on scene modifications and assumptions such as Lambertian reflection for all interior surfaces.

The method is employed to measure control of daylight glare by a CFS that shades sun-light by retro-reflection, and partially deflects it toward the ceiling in the upper window zone.

##### 4.2. Results and discussion

Figure 3 shows an exemplary falsecolor sequence from an annual set of imagery generated by the proposed method. The deflection of sun-light toward the ceiling is replicated as well as a vertical highlight on the system occurring when the sun is in the field of view, even if mitigated by the CFS. Since noise affects darker image regions most where photon density is low, and the color scale is adjusted to cover the highlights, artefacts are not apparent in this illustration. As most luminance-based metrics require accurate pixel values in bright image regions, but are not sensitive to low-frequency noise such as that introduced by the PHOTON MAP in darker regions, the results are assumed to be valid for visual comfort assessments e.g. employing Daylight Glare Probability (DGP) as a measure for glare. This possible application is illustrated by Figure 4.

## 5. Conclusions

The PHOTON MAP has been demonstrated as an efficient and valid means to sample data-driven BSDF models in daylight simulation. This holds true in particular for the generation of imagery for single points-in-time under sunny sky conditions, when the forward-distribution starts from the known sun direction rather than finding it through stochastic backward sampling. In an exemplary application of the method, computation times only for the image synthesis decreased by at least 98%, and by more than 99% when precomputed photons replaced the gathering of global photons. The fast image synthesis lowers the barrier to utilize luminance-based metrics, and even allows to generate imagery e.g. for multiple views by reusing the photon maps, extending the coverage of visual comfort evaluations into the spatial domain.

Due to the high efficacy of the algorithm when applied to narrow or highly directional light sources, the PHOTON MAP lends itself as a general technique to compute the direct solar component in CBDM. While the inevitable direct visualization of photons with the OoC storage introduces noise, this is considered a minor concern since most annual simulations are performed for the evaluation by performance metrics, which are insensitive to such artefacts.

One inherent limitation of the PHOTON MAP is its scalability. Other than further increasing the amount of photons, *progressive photon mapping* and balancing the bandwidth in photon gathering with the photon emission seems to be a worthwhile field of future research. The application of precomputed photons in CBDM would be another promising approach to reduce simulation times and the size of photon maps.

## Acknowledgments

Thanks to my colleague Roland Schregle and to Greg Ward for their advice and guidance, and to Tuğçe Kazanasmaz and Stephen Wittkopf for their valuable feed-back on my PhD research at Izmir Institute of Technology. The LCP was kindly provided by Ian Edmonds and Chantal Basurto-Dàvila. This research was funded by the Swiss Innovation Agency Innosuisse, contract #1155000149, as part of the Swiss Competence Center for Energy Research SCCER FEEB&D, and by the Swiss National Science Foundation under the grant “Light fields in climate-based daylight modeling for spatio-temporal glare assessment” (SNSF #200021\_179067).

## References

- [1] Grobe L O 2018 *Energy and Buildings* **162** 121–133
- [2] Molina G, Bustamante W, Rao J, Fazio P and Vera S 2015 *Journal of Building Performance Simulation* **8** 216–225
- [3] Ward G, Mistrick R, Lee E, McNeil A and Jonsson J 2011 *Leukos* **7** 241–261
- [4] McNeil A 2011 On the sensitivity of daylight simulations to the resolution of the hemispherical basis used to define bidirectional scattering distribution functions Tech. rep. DOE Technical Memo
- [5] Ward G, Kurt M and Bonneel N 2014 Reducing anisotropic BSDF measurement to common practice *Eurographics Workshop on Material Appearance Modeling* ed Klein R and Rushmeier H (The Eurographics Association) ISSN 2309-5059
- [6] Subramaniam S 2017 Daylighting simulations with Radiance using matrix-based methods Tech. rep. Lawrence Berkeley National Laboratory
- [7] Lee E S, Geisler-Moroder D and Ward G 2018 *Solar Energy* **160** 380–395
- [8] Jensen H W 2001 *Realistic image synthesis using photon mapping* (AK Peters / CRC Press)
- [9] Schregle R 2004 *Daylight simulation with photon maps* Ph.D. thesis Universitaet des Saarlandes
- [10] Schregle R, Grobe L O and Wittkopf S K 2015 *Solar Energy* **114** 327–336
- [11] Bauer C and Wittkopf S 2016 *Journal of Facade Design and Engineering* **3** 253–272
- [12] Bellia L, Pedace A and Fragliasso F 2015 *Solar Energy* **122** 249 – 263
- [13] Schregle R, Grobe L O and Wittkopf S 2016 *Journal of Building Performance Simulation* **9** 620–632
- [14] Apian-Bennewitz P 2010 New scanning gonio-photometer for extended BRDF measurements *Proceedings SPIE vol 7792 Reflection, Scattering, and Diffraction from Surfaces II* (Brussels, B: International Society for Optics and Photonics) pp 77920O–77920O
- [15] Christensen P H 1999 *Journal of Graphics Tools* **4** 1–10